Crystals for Homogeneous EM Calorimetry

Video of the lecturer

In crystals the light emission is related to the crystal structure of the material. Incident charged particles create electron-hole pairs and photons are emitted when electrons return to the valence band.

The incident electron or photon is completely absorbed and the produced amount of light, which is reflected through the transparent crystal, is measured by photomultipliers (PM) or solid state photon detectors (SiPM)

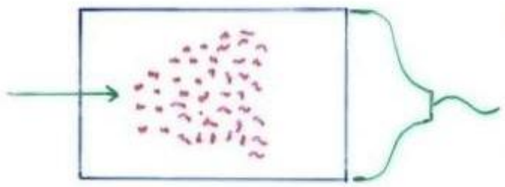

Measuring the Photons produced by the collision of the $e^{\pm}$ with atom electrons of the material

Crystals for Homogeneous EM Calorimetry

Video of the lecturer

	NaI(Tl)	CsI(Tl)	CsI	BGO	$PbWO_4$
Density (g/cm^3)	3.67	4.53	4.53	7.13	8.28
X_0 (cm)	2.59	1.85	1.85	1.12	0.89
R_M (cm)	4.5	3.8	3.8	2.4	2.2
Decay time (ns)	250	1000	10	300	5
slow component			36		15
Emission peak (nm)	410	565	305	410	440
slow component			480		
Light yield γ/MeV	4×10^4	5×10^4	4×10^4	8×10^3	1.5×10^2
Photoelectron yield (relative to NaI)	1	0.4	0.1	0.15	0.01
Rad. hardness (Gy)	1	10	10^3	1	10^5

Babar@PEPII, 10ms interaction rate, good light yield, good S/N

KTeV@Tevatron, High rate, Good resolution

L3@LEP, 25us bunch crossing, Low radiation dose

CMS@LHC, 25ns bunch crossing, high radiation dose

Crystals for Homogeneous EM Calorimetry

Video of the lecturer

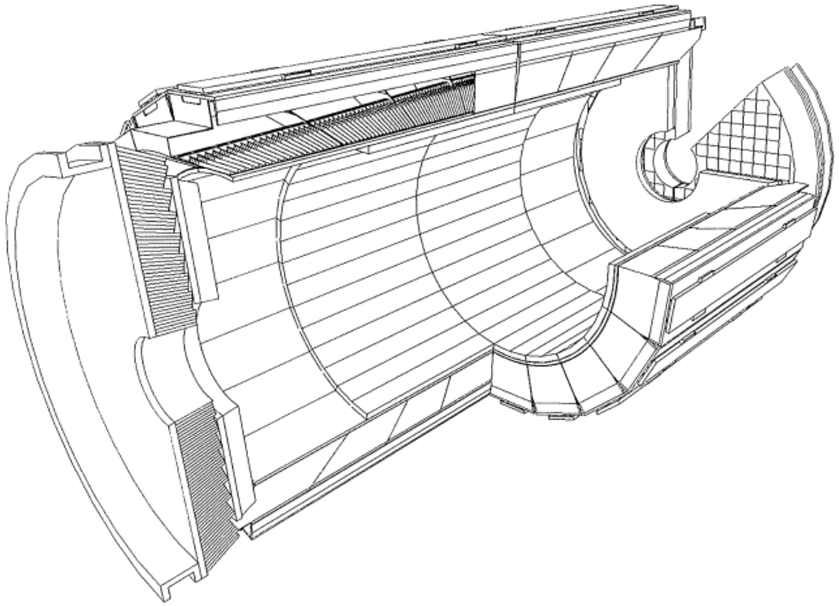

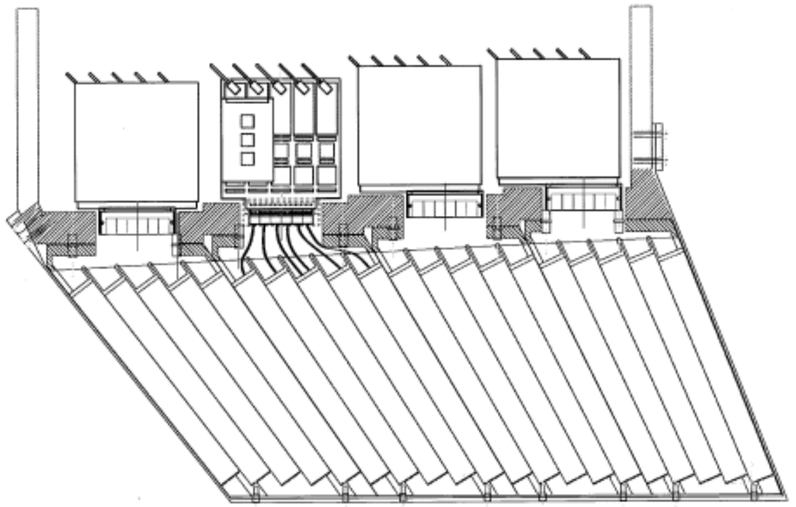

Fig. 2. Longitudinal drawing of module 2, showing the structure and the front-end electronics layout.

Noble Liquids for Homogeneous EM Calorimetry

	Ar	Kr	Xe
Z	18	36	58
A	40	84	131
X_0 (cm)	14	4.7	2.8
R_M (cm)	7.2	4.7	4.2
Density (g/cm^3)	1.4	2.5	3.0
Ionization energy (eV/pair)	23.3	20.5	15.6
Critical energy ϵ (MeV)	41.7	21.5	14.5
Drift velocity at saturation (mm/μs)	10	5	3

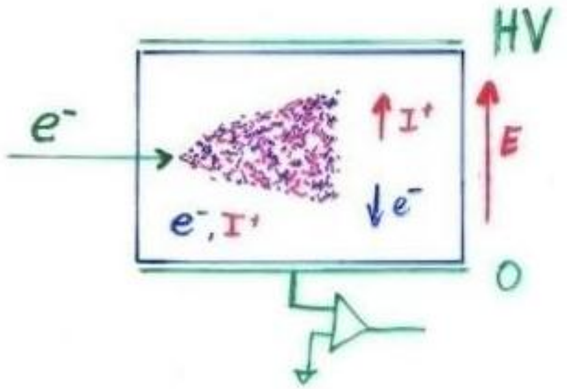

Video of the lecturer

When a charge particle traverses these materials, about half the lost energy is converted into ionization and half into scintillation.

The best energy resolution would obviously be obtained by collecting both the charge and light signal. This is however rarely done because of the technical difficulties to extract light and charge in the same instrument.

Krypton is preferred in homogeneous detectors due to small radiation length and therefore compact detectors. Liquid Argon is frequently used due to low cost and high purity in sampling calorimeters.

Noble Liquids for Homogeneous EM Calorimetry

Video of the lecturer

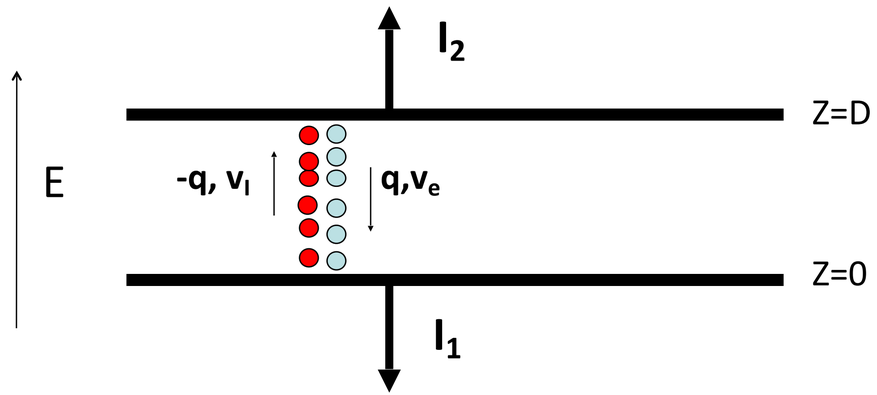

E.g. Liquid Argon, 5mm/μs at 1kV/cm, 5mm gap → 1μs for all electrons to reach the electrode.

The ion velocity is 10^3 to 10^5 times smaller → doesn't contribute to the signal for electronics of μs integration time.

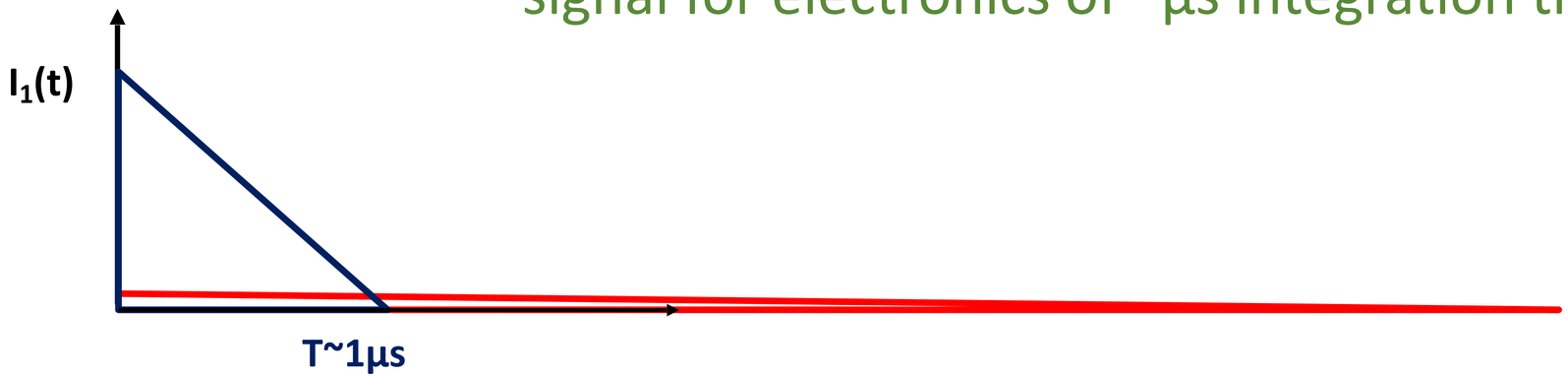

Homogeneous EM Calorimeters, Examples

Video of the lecturer

NA48 Liquid Krypton
2cmx2cm cells
X_0 = 4.7cm
125cm length ($27X_0$)
ρ = 5.5cm

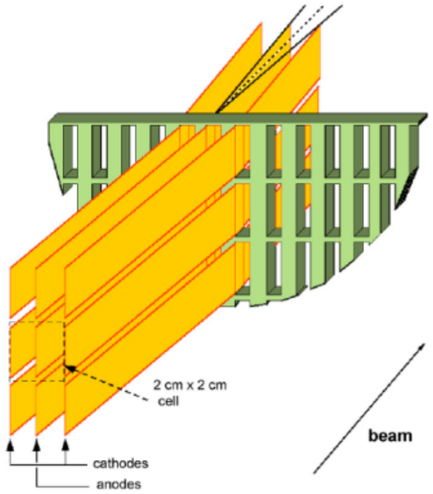

KTeV CsI
5cmx5cm and
X_0 = 1.85cm
2.5cmx2.5cm crystals
50cm length ($27X_0$)
ρ = 3.5cm

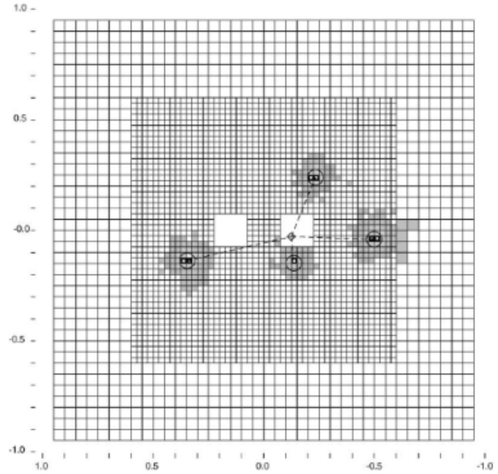

Fig. 1. Schematic of the KTeV CsI Calorimeter showing the cluster energy profiles due to four photons.

NA48 Experiment at CERN and KTeV Experiment at Fermilab, both built for measurement of direct CP violation. Homogenous calorimeters with Liquid Krypton (NA48) and CsI (KTeV). Excellent and very similar resolution.

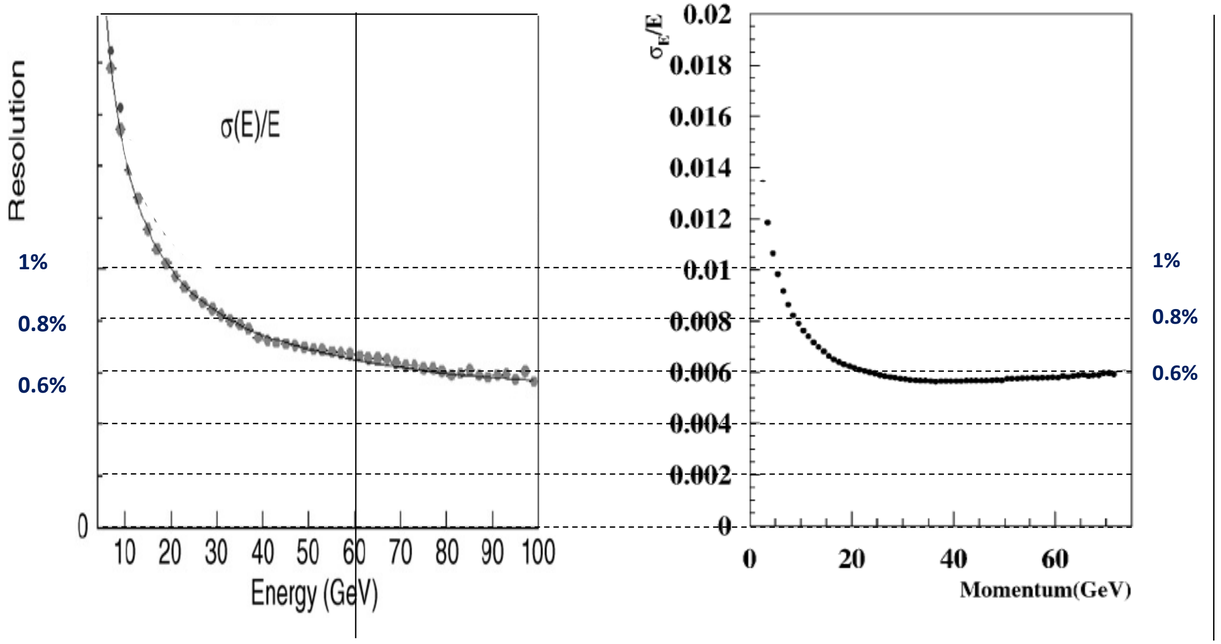

Energy Resolution of Calorimeters

Video of the lecturer

Stochastic term:
Fluctuations related to the physics development of the shower.

Noise term:
From electronics noise of the readout chain. For constant electronics noise → double signal = double S/N

Constant term:
Instrumental effects that cause variations of the calorimeter response with the particle impact point.

$$\frac{\sigma}{E} = \frac{a}{\sqrt{E}} \oplus \frac{b}{E} \oplus c$$

Add in squares

For homogeneous calorimeters the noise term and constant term become dominant.

For sampling calorimeters the stochastic term, then called ‘sampling’ term becomes dominant.

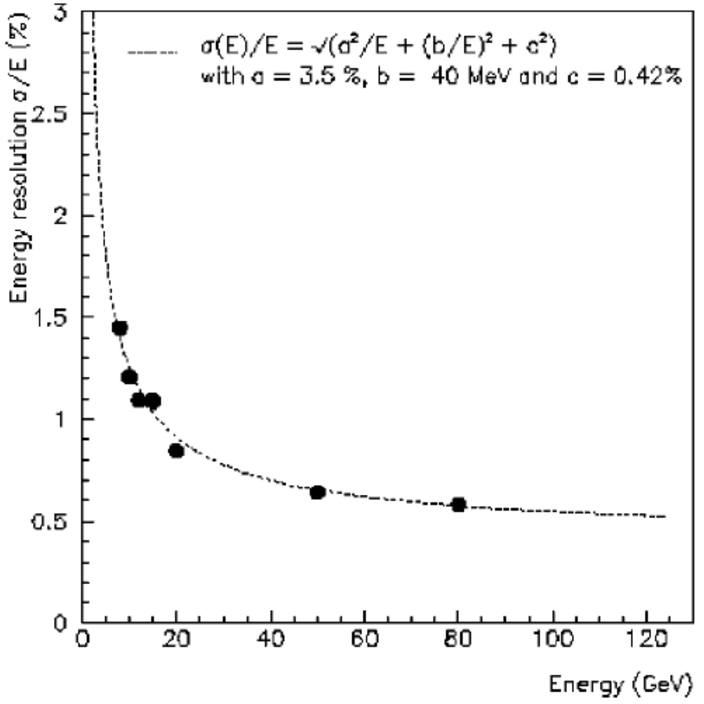

FIG. 3. Fractional electron energy resolution as a function of energy measured with a prototype of the NA48 liquid krypton electromagnetic calorimeter (NA48 Collaboration, 1995). The line is a fit to the experimental points with the form and the parameters indicated in the figure.

Sampling Calorimeters

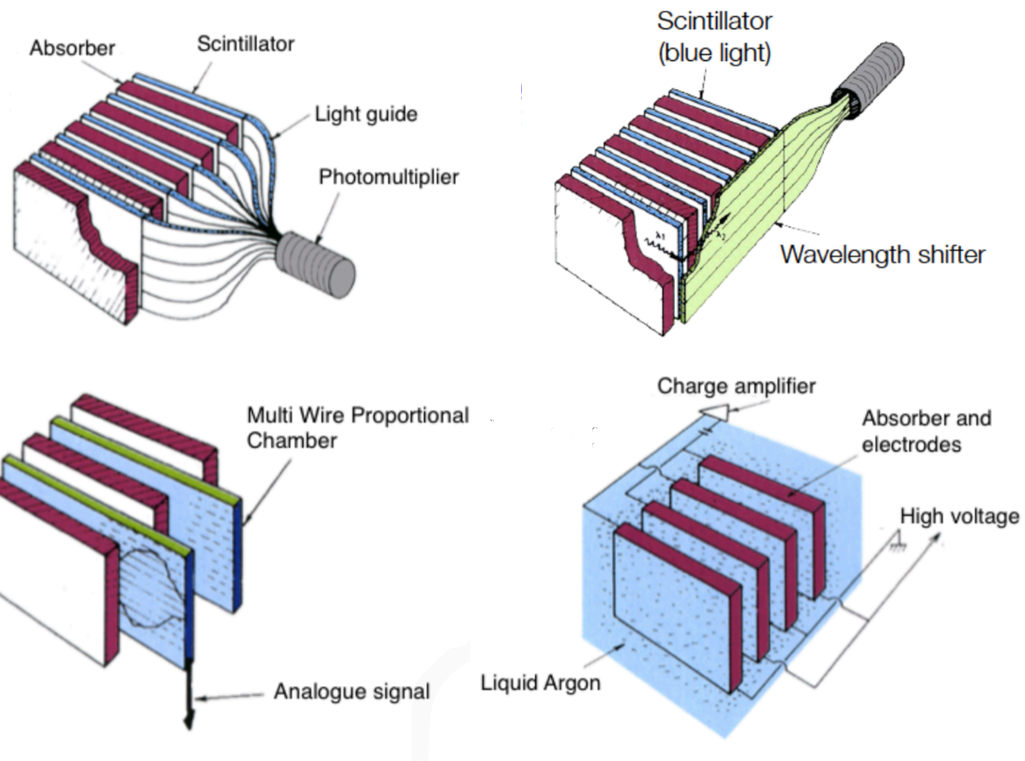

Alternation of "passive" absorber plates and "active" readout sections

Advantage:

- optimum choice of absorber material
- optimum choice of signal readout
- compact and cheap construction

"passive": Pb, Fe…

"active": Scintillator (signal → Photons)

Noble Liquid, e.g. Ar (Signal → e^-, I^-)

Wire Chambers (Signal → e^-, I^+)

Emulsions (Signal —> tracks)

Video of the lecturer

Energy resolution of sampling calorimeters is in general worse than that of homogeneous calorimeters, owing to the sampling fluctuations – the fluctuation of ratio of energy deposited in the active and passive material.

The resolution is in the range 5-20%/Sqrt[E(GeV)] for EM calorimeters. On the other hand they are relatively easy to segment longitudinally and laterally and therefore they usually offer better space resolution and particle identification than homogeneous calorimeters.

Active medium can be scintillators, solid state detectors, emulsion films, gas detectors or liquids.

Sampling Fraction = Energy deposited in Active/Energy deposited in passive material.

Gas and Solid State Sampling Calorimeters

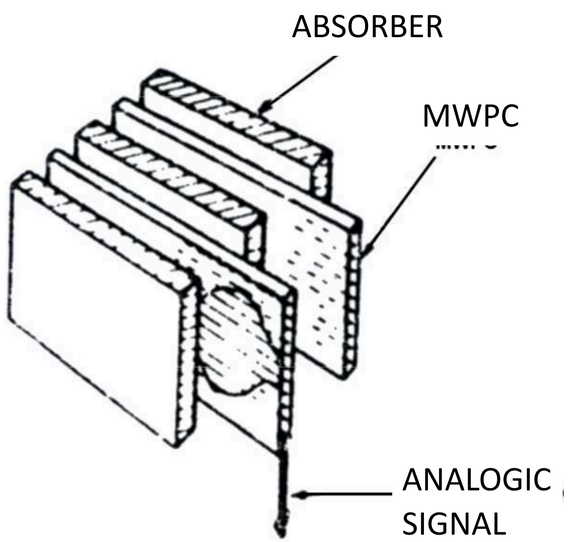

Gas sampling calorimeters have been widely employed at LEP because of their low cost and segmentation flexibility.

They are not well suited to present and future machines because of their modest EM energy resolution ~ 20%/Sqrt[E(GeV)].

Video of the lecturer

Solid state detectors as active readout medium use mostly silicon. The advantage is very high signal to noise ratio (large signals). Often used on a small scale as luminosity monitors.

The disadvantage is the high cost, preventing large calorimeters, and modest radiation resistance.

Scintillator Sampling Calorimeters

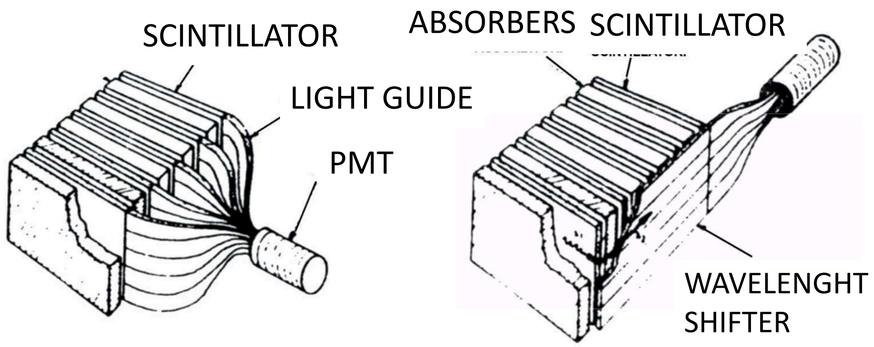

Wavelength shifters absorb photons from the scintillators and emit light at a longer wavelength which does not go back into the scintillator but is internally reflected along the readout plate to the photon detector → compact design.

Video of the lecturer

A large number of sampling calorimeters use organic scintillators arranged in fibers or plates.
The drawbacks are that the optical readout suffers from radiation damage and non-uniformities at various stages are often the source of a large constant term.

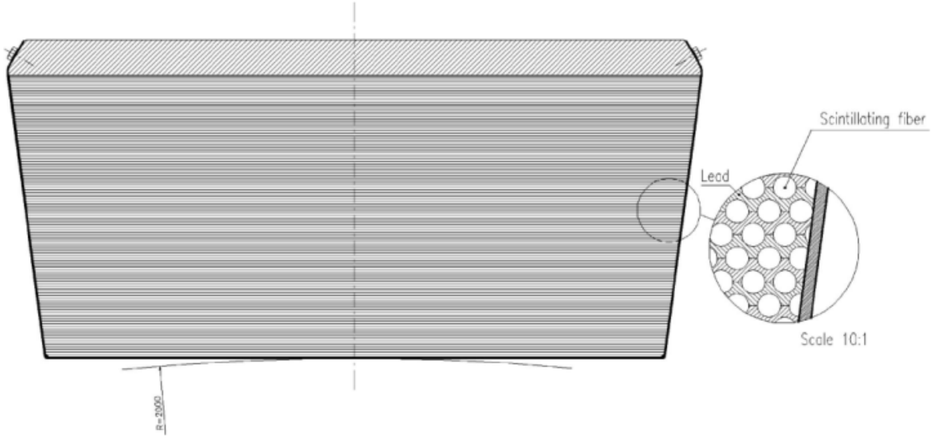

FIG. 13. Schematic layout of the barrel part of the KLOE electromagnetic calorimeter (Antonelli *et al.*, 1995).

KLOE EM calorimeter:

$$\frac{5\%}{\sqrt{E(GeV)}}$$

Liquid Sampling Calorimeters

Video of the lecturer

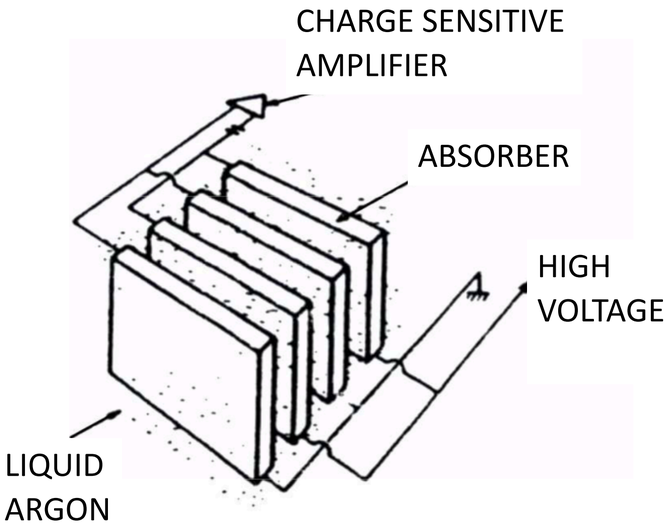

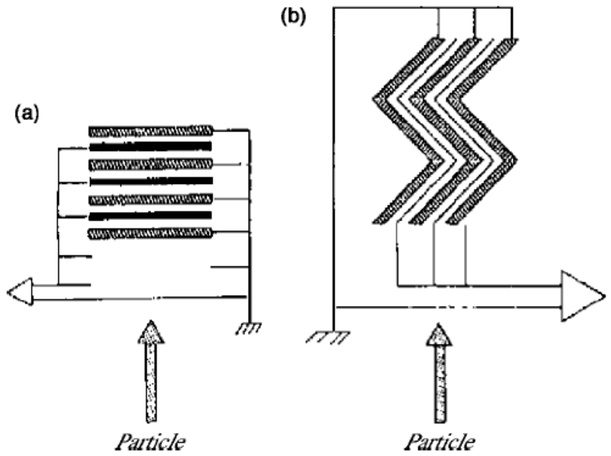

FIG. 15. Schematic view of a traditional sampling calorimeter geometry (a) and of the accordion calorimeter geometry (b).

Liquids at room temperature do not require cryogeny but are characterized by poor radiation resistance and suffer from purity problems

→Noble liquids at cryogenic temperatures.

The advantages are operation in 'ion chamber mode', i.e. deposited charge is large and doesn't need multiplication, which ensures better uniformity compared to gas calorimeters that need amplification.

They are relatively uniform and easy to calibrate because the active medium is homogeneously distributed inside the volume. They provide good energy resolution (e.g. ATLAS 10%/Sqrt[E(GeV)])

And stable operation with time.

They are radiation hard.

With the standard liquid argon sampling calorimeters the alternating absorber and active layers are placed perpendicular to the direction of the incident particle.

→ Long cables are needed to gang together the readout electrodes, causing signal degradation, dead spaces between the calorimeter towers and therefore reduced hermeticity.

Liquid Argon Sampling Calorimeters

Video of the lecturer

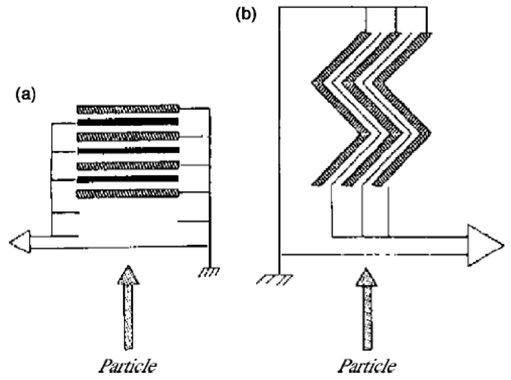

FIG. 15. Schematic view of a traditional sampling calorimeter geometry (a) and of the accordion calorimeter geometry (b).

For the ATLAS LAr Calorimeter this was solved by placing the absorbers in an accordion geometry parallel to the particle direction and the electrodes can be read out from the 'back side'.

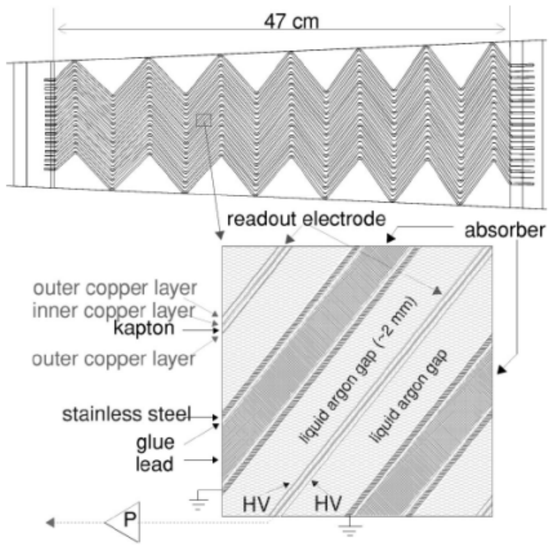

ATLAS: Lead layers of 1.1-2.2mm, depending on the rapidity region, separated by 4mm liquid Argon gaps.

Test beam results have shown:

$$\frac{10\%}{\sqrt{E(GeV)}} \cdot \frac{0.25}{E(GeV)} \cdot 0.3\%$$

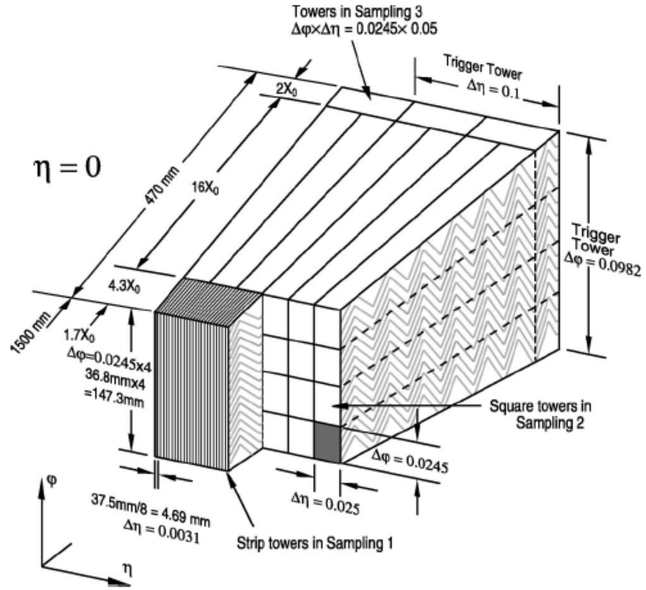

FIG. 17. Schematic view of the segmentation of the ATLAS electromagnetic calorimeter.

Emulsion Cloud Chamber: a peculiar type of sampling calorimeter

Video of the lecturer

One brick:
- 57 emulsion films
- 56 Pb plates
- a box with a removable pair of films called Changeable Sheets

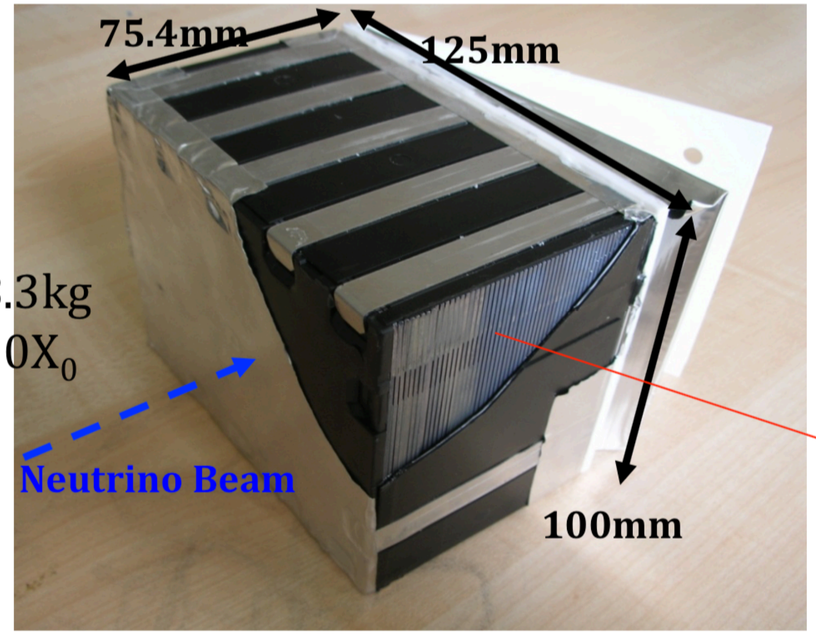

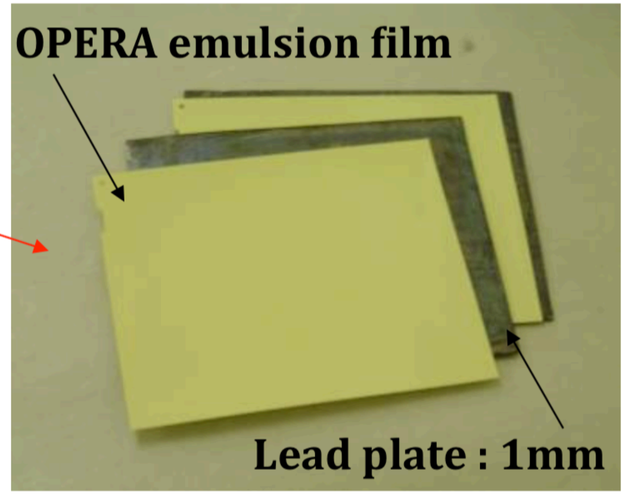

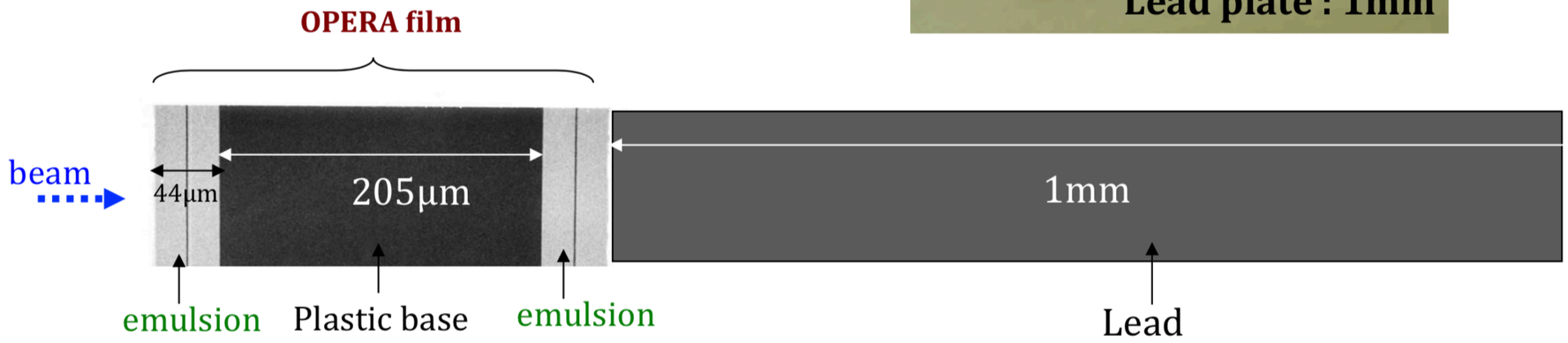

Electromagnetic showers as seen in an Emulsion Cloud Chamber: e/π^0 separation

Video of the lecturer

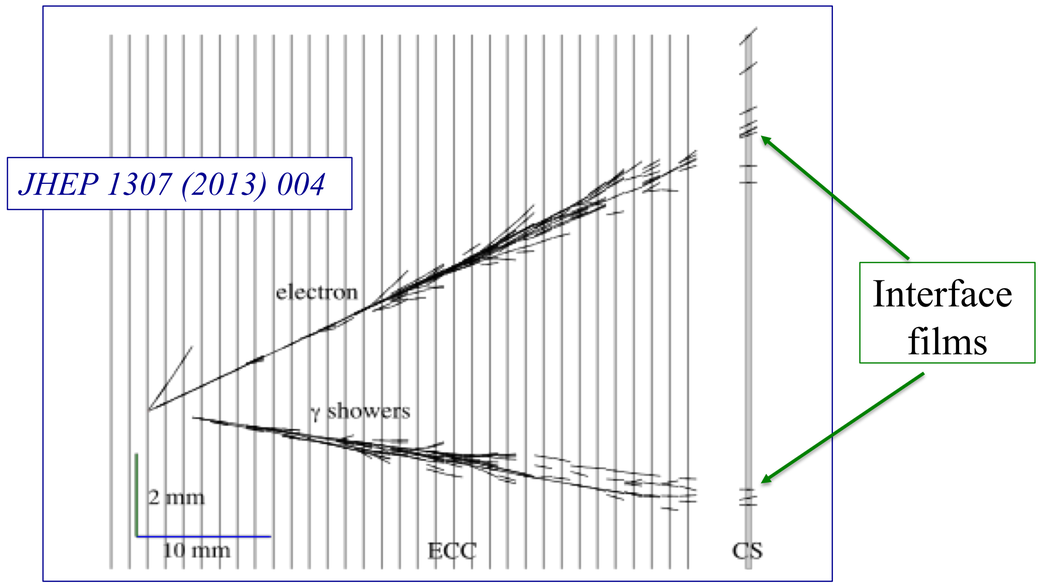

$$\Sigma \Delta E_{invis} + \Sigma \Delta E_{vis} = E_{invis} + E_{vis} = E_{absorbed}$$

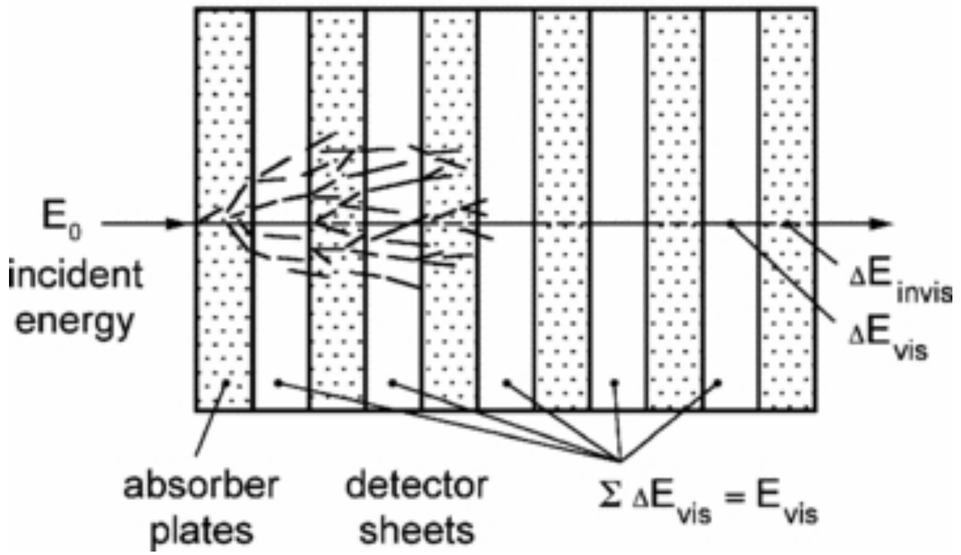

High sampling frequency, 6 active layers every X^0

—> high spatial resolution —> high purity in e/π^0 separation

Electron neutrino interaction with a π^0

Video of the lecturer

Transverse plane

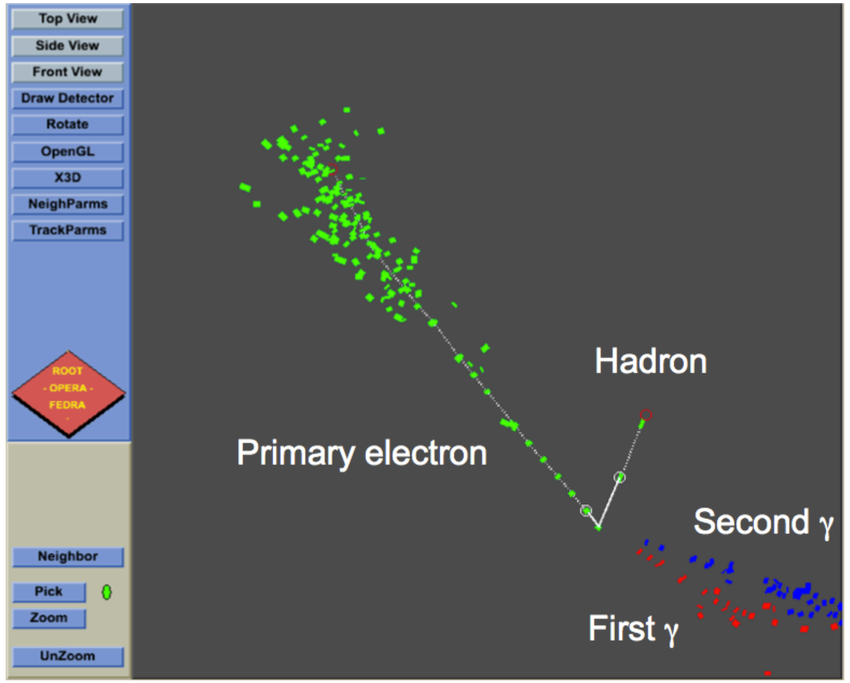

Side view

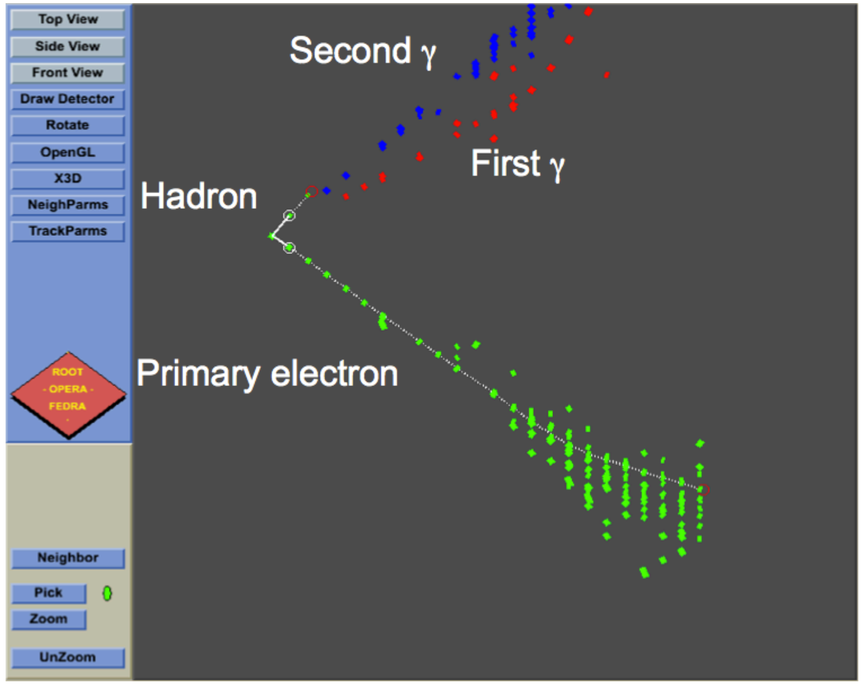

Algorithms for shower and energy reconstruction

Video of the lecturer

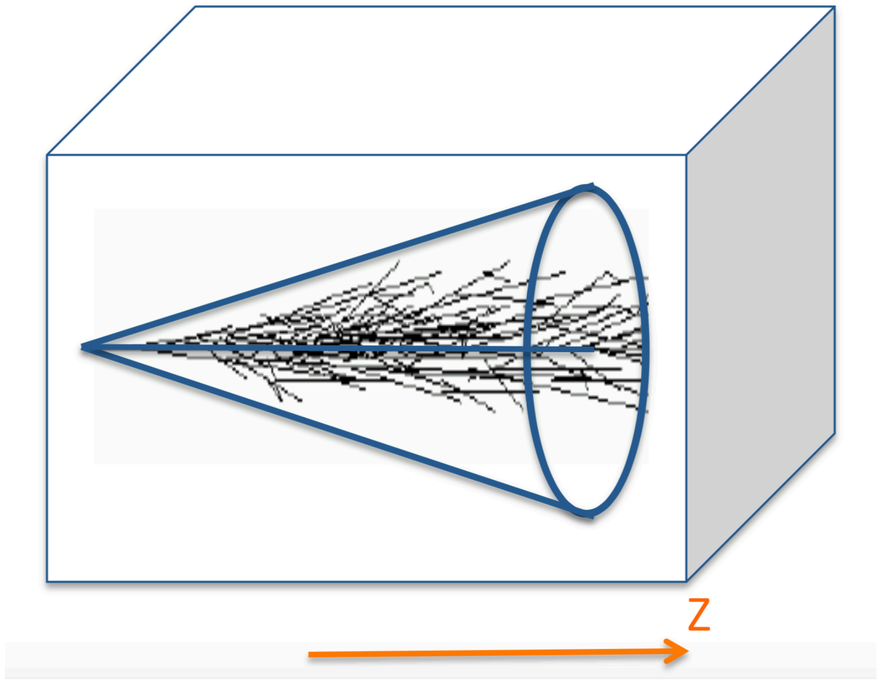

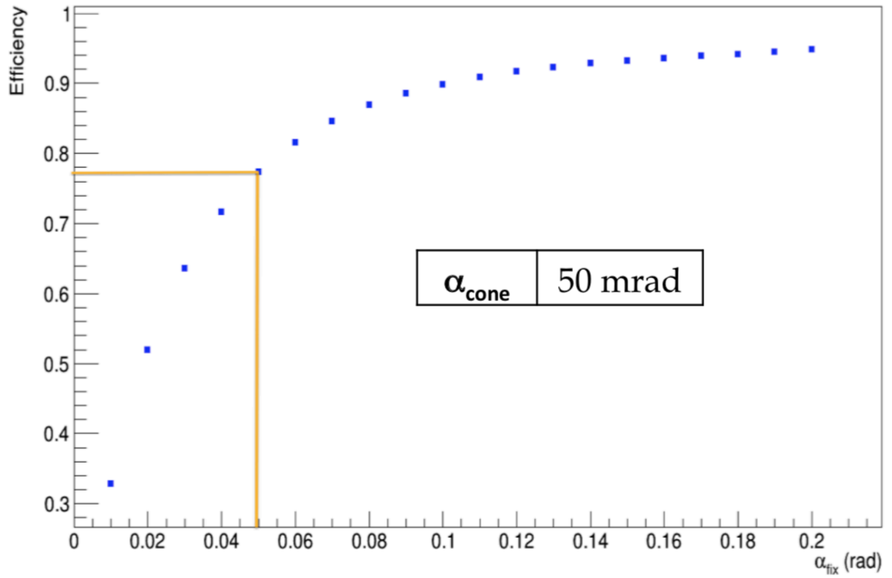

$$\text{Efficency} = \frac{\text{Number of the tracks inside the cone for a given opening angle}}{\text{Total Number of tracks related to the shower}}$$

Variables Used to discard the Instrumental Background

Video of the lecturer

1. Alpha:

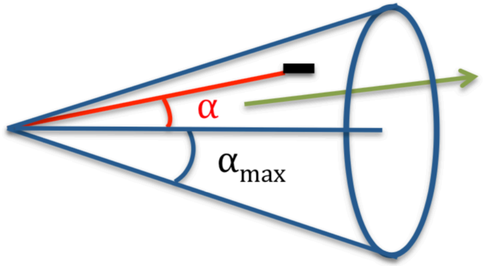

Alpha is calculated for all BTs

α_{max} = 50 mrad

$0 < \alpha < 50$ mrad

2. Impact Parameter divided by the distance from the decay vertex:

$$IPA = \frac{IP}{\Delta z}$$

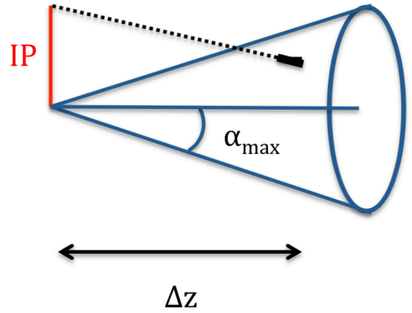

3, 4. ΔSx, ΔSy:

- $\Delta Sx = Sx_e - Sx_i$
- $\Delta Sy = Sy_e - Sy_i$

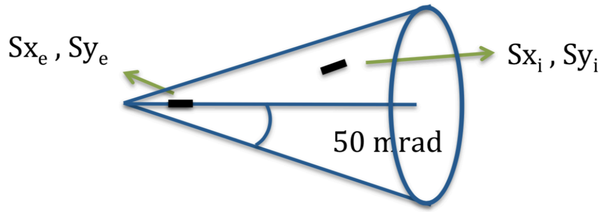

5. χ^2:

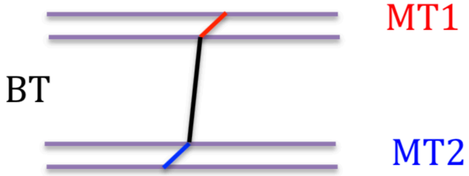

Different performance in different zones

Video of the lecturer

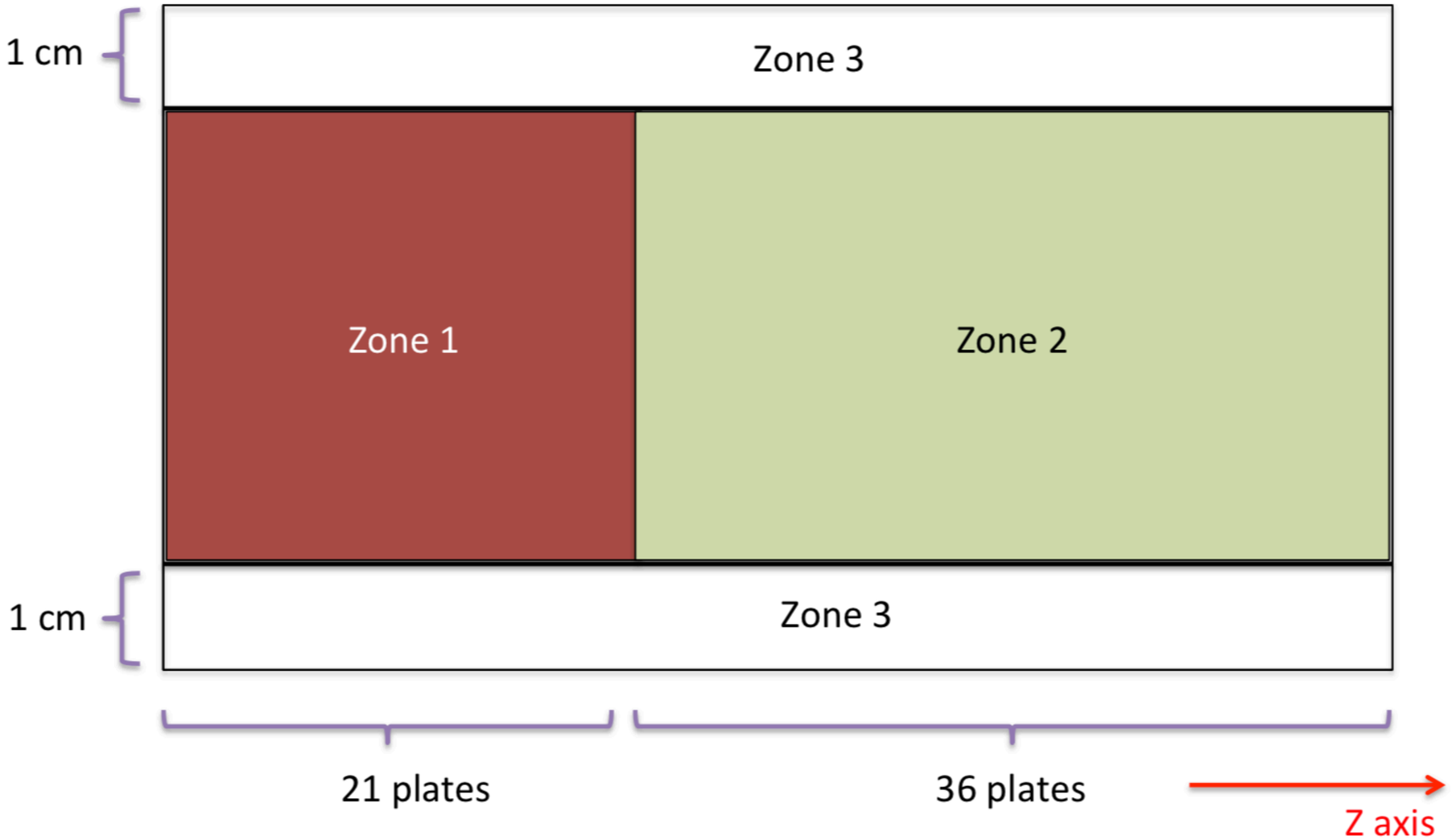

Variables used in the analysis of Zone 1 events

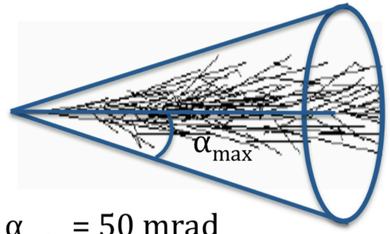

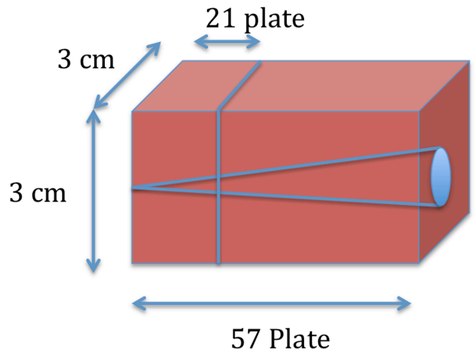

Video of the lecturer

A cone with opening angle 50 mrad is defined, starting from the decay point for the τ→e decays, and from the primary vertex for ν_e events.

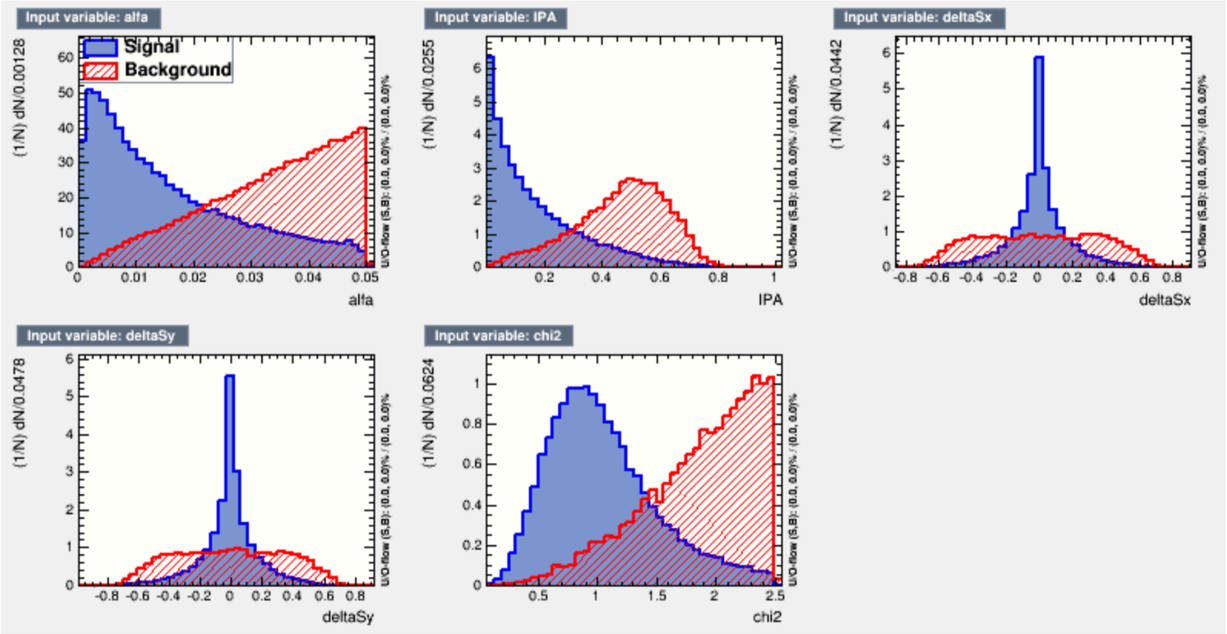

Energy Resolution

Video of the lecturer

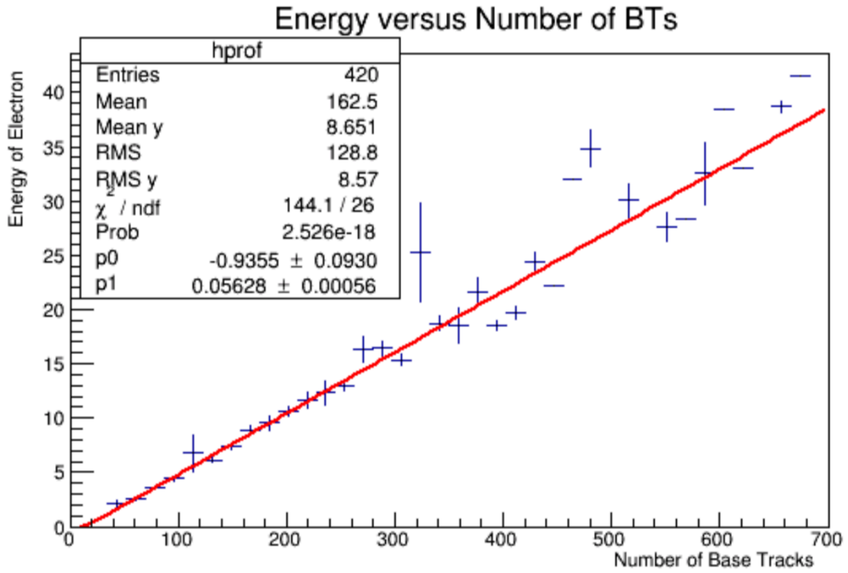

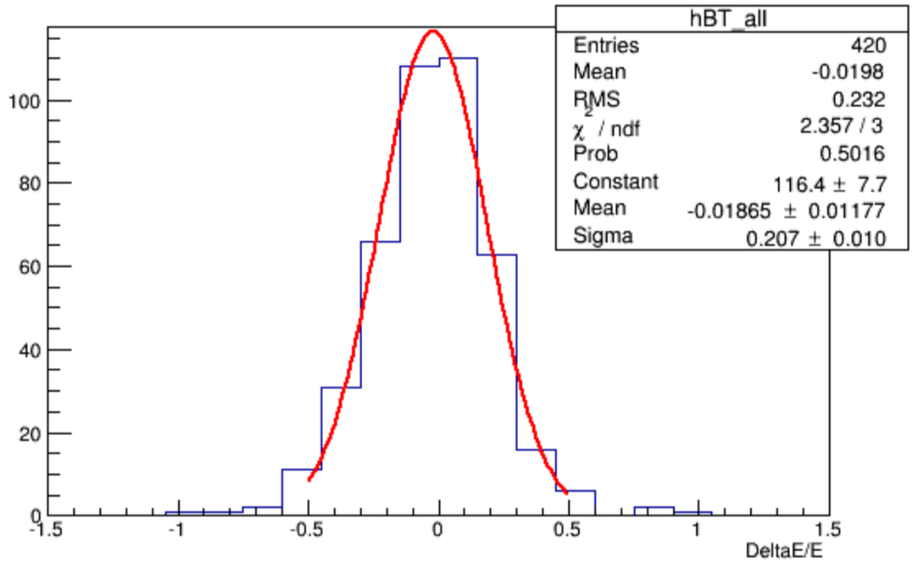

$$\frac{\Delta E}{E} = \frac{E_{true} - E_{meas}}{E_{true}}$$

$$\sigma = 21\,\%$$

Average number of BTs per event (Signal) = 160

Average number of BTs per event (BG) = 17

Analysis extended to the downstream brick

Video of the lecturer

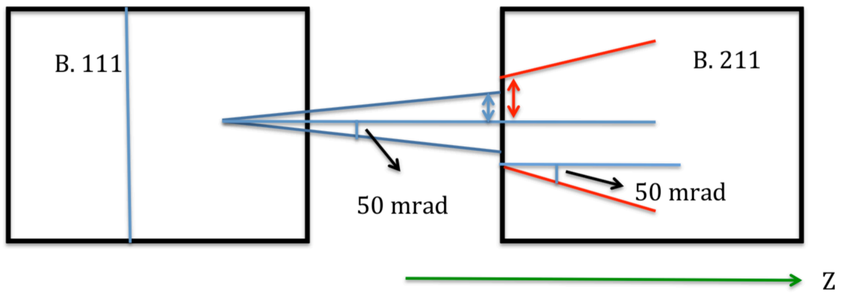

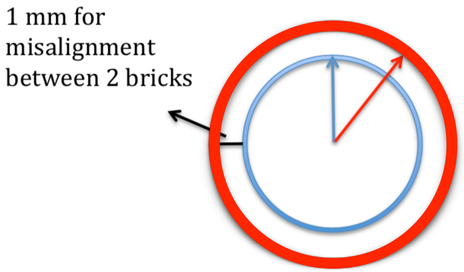

Gap between the 2 bricks (ED): Z = 5.3 cm

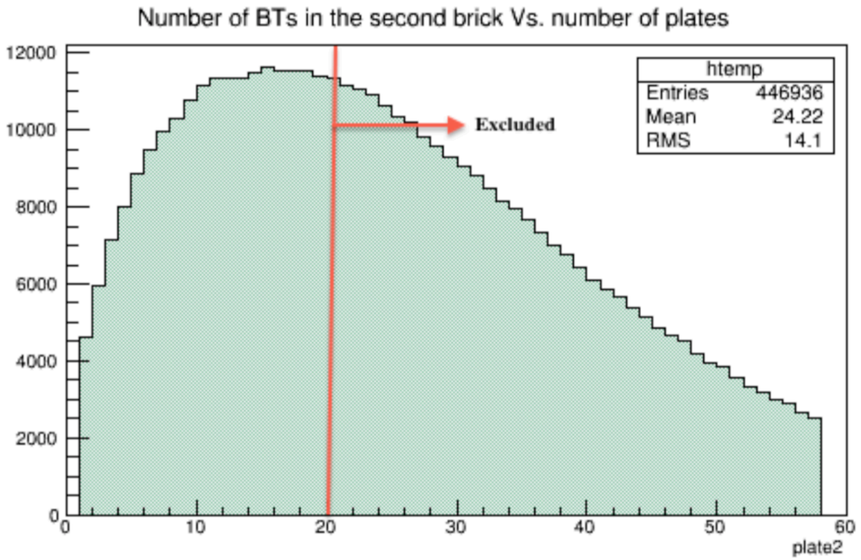

A volume of 20 films with a surface of 3x3 cm^2 each is scanned to estimate the background

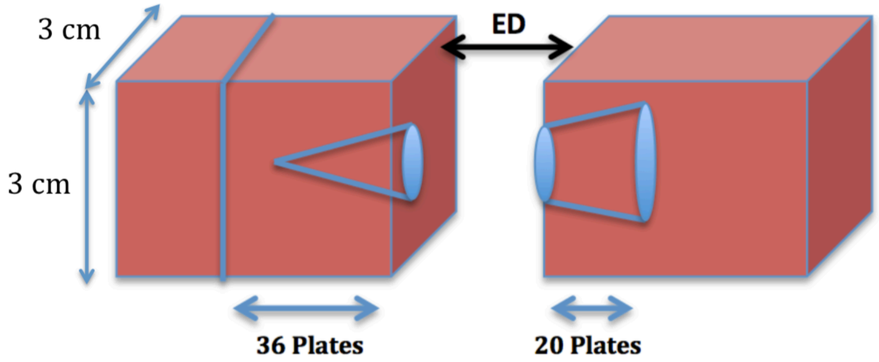

Resolution using the downstream brick

Video of the lecturer

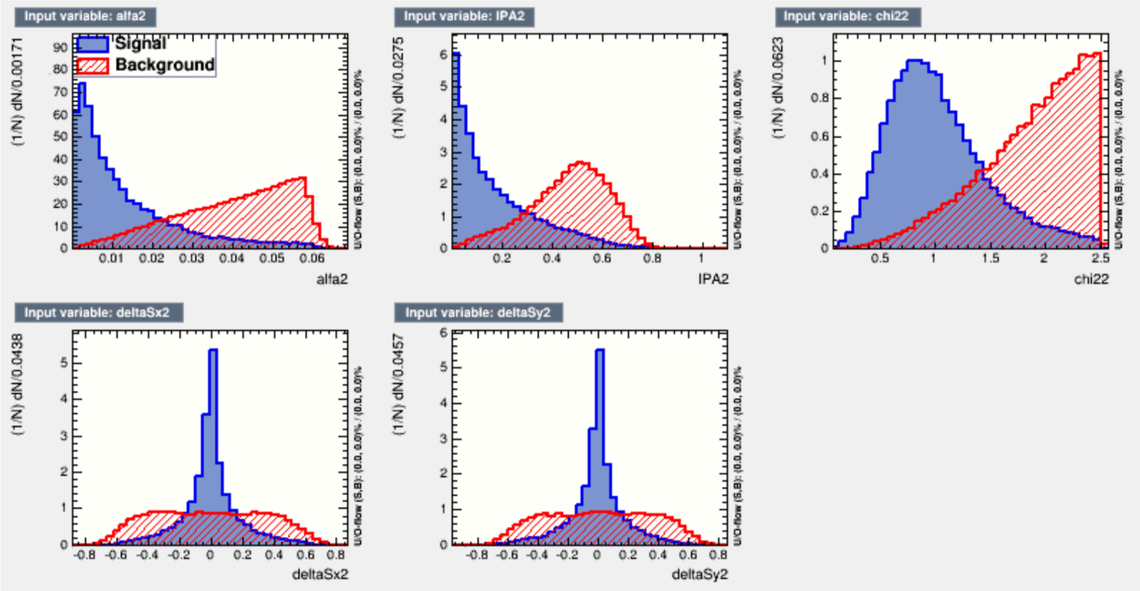

$$\frac{\Delta E}{E} = \frac{E_{true} - E_{meas}}{E_{true}} \qquad \sigma = 0.23$$

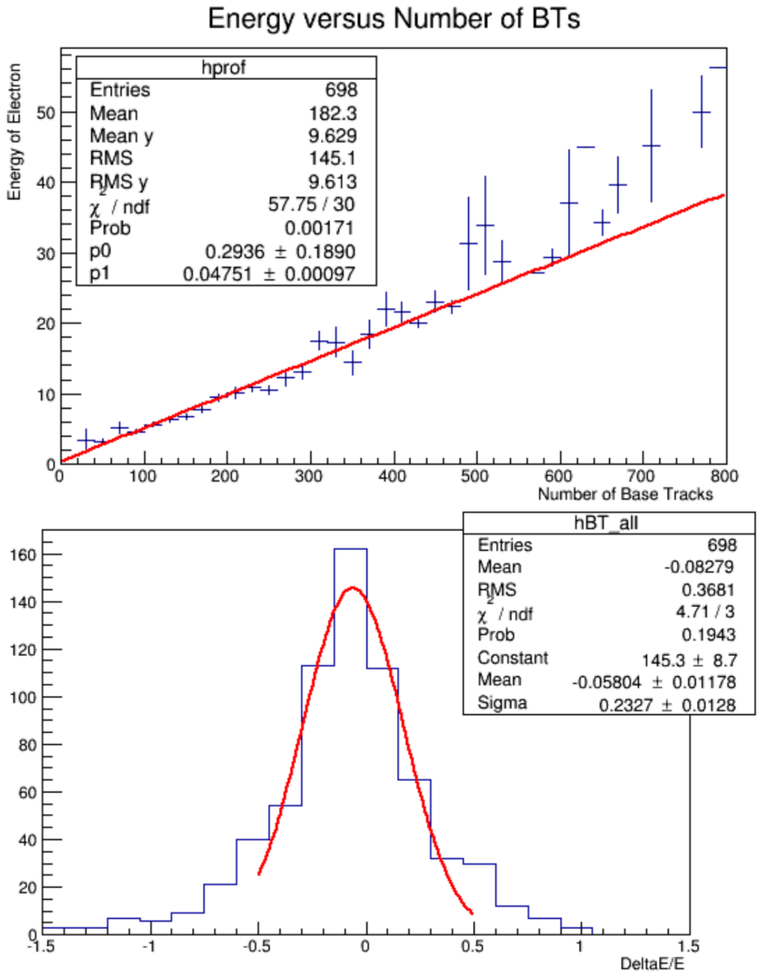

Average number of BTs per event (Signal) = 218

Average number of BTs per event (BG) = 18

Quiz

Video of the lecturer

Explain why the stochastic term in the relative energy resolution goes like $\frac{a}{\sqrt{E}}$

Explain the main features of an emulsion/lead chamber in terms of its calorimetric response.